IOP Publishing New J. Phys. 26 (2024) 033020 https://doi.org/10.1088/1367-2630/ad2d1d

New Journal of Physics
The open access journal at the forefront of physics

Deutsche Physikalische Gesellschaft DPG
IOP Institute of Physics

Published in partnership with: Deutsche Physikalische Gesellschaft and the Institute of Physics

OPEN ACCESS

RECEIVED
20 November 2023

REVISED
19 February 2024

ACCEPTED FOR PUBLICATION
26 February 2024

PUBLISHED
15 March 2024

PAPER

Quantum simulation of excited states from parallel contracted quantum eigensolvers

Carlos L Benavides-Riveros[1,*], **Yuchen Wang**[2], **Samuel Warren**[2] and **David A Mazziotti**[2,*]

[1] Pitaevskii BEC Center, CNR-INO and Dipartimento di Fisica, Università di Trento, I-38123 Trento, Italy
[2] Department of Chemistry and The James Franck Institute, The University of Chicago, Chicago, IL 60637, United States of America
[*] Authors to whom any correspondence should be addressed.

E-mail: damazz@uchicago.edu and cl.benavidesriveros@unitn.it

Keywords: excited states, quantum simulation, anti-Hermitian contracted Schrödinger equation, non-unitary transformations, wave function ansatz, contracted quantum eigensolver

Abstract

Computing excited-state properties of molecules and solids is considered one of the most important near-term applications of quantum computers. While many of the current excited-state quantum algorithms differ in circuit architecture, specific exploitation of quantum advantage, or result quality, one common feature is their rooting in the Schrödinger equation. However, through contracting (or projecting) the eigenvalue equation, more efficient strategies can be designed for near-term quantum devices. Here we demonstrate that when combined with the Rayleigh–Ritz variational principle for mixed quantum states, the ground-state contracted quantum eigensolver (CQE) can be generalized to compute any number of quantum eigenstates simultaneously. We introduce two *excited-state* (anti-Hermitian) CQEs that perform the excited-state calculation while inheriting many of the remarkable features of the original ground-state version of the algorithm, such as its scalability. To showcase our approach, we study several model and chemical Hamiltonians and investigate the performance of different implementations.

1. Introduction

Calculating physical properties of excited-state processes of quantum many-body systems is one of the most promising applications of near-term quantum computing [1–3]. Quantum devices are well suited to deal with many of the distinctive features of excited states such as their strong multiconfigurational character or the presence of conical intersections [4, 5]. So far, several quantum algorithms have been developed to approximate eigenstates of many-body Hamiltonians, including quantum phase estimation (QPE) [6, 7] and the variational quantum eigensolver (VQE) [8, 9]. VQE has also inspired several related approaches for excited states: The two dominant variants rely on either targeting specific states through adding nonorthogonal penalties to the Hamiltonian [10–14] or by building subspaces while ensuring orthogonality of the lowest-lying eigenstates [15, 16]. Yet, QPE requires circuit depths beyond what is currently achievable, and VQE relies on high-dimensional classical optimization, which has computational costs that scale rapidly with the system size [17].

Quantum algorithms like QPE and VQE are designed to solve the Schrödinger equation (SE). However, more efficient quantum simulations can be performed if, instead of the standard SE, its contraction (or projection) is solved directly on a quantum computer [18]. When solving the corresponding contracted Schrödinger equation (CSE) the prepared wave function ansatz only requires two-body terms, regardless of the number of electrons or orbitals, ensuring the scalability of the algorithm [19]. While initially designed to explore ground states of molecular systems [19], quantum eigensolvers based on the CSE have been recently extended to excited states by using the variance of the energy as the cost function [20] or by deflating the CSE to ensure the orthogonality of the eigenstates [21]. However, these methods compute the eigenstates individually and therefore the circuit must be run for each desired excited state.

The goal of this work is to demonstrate that when combined with the Rayleigh–Ritz variational principle for mixed quantum states, the CSE can be straightforwardly generalized for the simultaneous (or parallel) calculation of a bundle of lowest eigenstates. Our main result is a novel excited-state quantum algorithm that employs the main features of the ground-state contracted quantum eigensolver (CQE), thus retaining its favorable scaling. Here we focus on the anti-Hermitian portion of the CSE which has been shown to render accurate approximations for ground-state calculations [22], but our results can be generalized to include its Hermitian part. In the same way, we focus on fermionic systems but our derivations equally hold for bosons.

The remainder of this paper is organized as follows: For completeness, we first introduce both the CSE and the Rayleigh–Ritz variational principle for ensembles, on which our algorithm is based. Next, we generalize the basic equations of the ground-state CQE to excited states and discuss the resulting quantum algorithm. We then present our CQEs, discuss different methods of implementing them on a quantum computer, and perform several numerical experiments. The paper ends with some conclusions and a discussion about potential future research directions.

2. Theory

After we review the CSE and the Rayleigh–Ritz variational principle for mixed states in sections 2.1 and 2.2, we derive an anti-Hermitian CSE (ACSE) for mixed states in section 2.3 and a quantum algorithm based on this mixed-state ACSE in section 2.4, which can solve for multiple excited states simultaneously.

2.1. Contracted SE

The SE of an electronic system governed by a Hamiltonian $\hat{H}$ reads:

$$\left(\hat{H} - E_\nu\right)|\psi_\nu\rangle = 0. \tag{1}$$

The two-body operator $\hat{\Gamma}^{pq}_{st} \equiv \hat{f}^\dagger_p \hat{f}^\dagger_q \hat{f}_t \hat{f}_s$, where $\hat{f}^\dagger_p / \hat{f}_p$ are fermionic creation/annihilation operators, followed by the vector $\langle\psi_\nu|$, can be applied on the left of the SE in equation (1) to obtain the CSE:

$$\langle\psi_\nu|\hat{\Gamma}^{pq}_{st}\left(\hat{H} - E_\nu\right)|\psi_\nu\rangle = 0. \tag{2}$$

Both the CSE in equation (2) and the SE in equation (1) have an *equivalent* set of pure-state solutions [23–25]: while the SE clearly implies the CSE, the opposite direction is provable by showing that (2) implies the eigenstate condition of zero variance (i.e. $\langle\psi_\nu|(\hat{H} - E_\nu)^2|\psi_\nu\rangle = 0$) which in turn implies the SE. Notice that equation (2) can be written as the sum of two terms (a commutator and anti-commutator) [26, 27]:

$$\langle\psi_\nu|\left\{\hat{\Gamma}^{pq}_{st}, \left(\hat{H} - E_\nu\right)\right\}|\psi_\nu\rangle + \langle\psi_\nu|\left[\hat{\Gamma}^{pq}_{st}, \hat{H}\right]|\psi_\nu\rangle = 0\,. \tag{3}$$

It is well-known that solving only the anti-Hermitian portion of this equation, i.e.

$$\langle\psi_\nu|\left[\hat{\Gamma}^{pq}_{st}, \hat{H}\right]|\psi_\nu\rangle = 0 \tag{4}$$

gives accurate results both for ground bosonic [28] and ground and excited electronic [20, 21] states. Although the ACSE, unlike the CSE, does not rigorously imply the SE [19], it contains roughly half of the degrees of freedom in the CSE, and hence, provides a stringent necessary condition for satisfaction of the SE. Practically, we find that solving the ACSE tends to generate an exact solution of the SE [20, 21]. Moreover, since equation (4) can be interpreted as the residual of a certain cost function, this ACSE immediately suggests the type of ansatz that can be used to guess the form of the eigenstate $|\psi_\nu\rangle$ (see below).

2.2. Variational principle for ensembles

The Rayleigh–Ritz variational principle is a powerful tool routinely used to study eigenstates of quantum many-body systems [29]. Its generalization to mixed quantum states establishes an upper bound for the weighted ensemble energy of the K lowest eigenstates of a Hamiltonian, $\hat{H}$ [30]:

$$\mathrm{Tr}\left[\rho(\boldsymbol{w})\hat{H}\right] \geqslant \sum_{\nu=0}^{K-1} w_\nu E_\nu, \tag{5}$$

where $\rho(\boldsymbol{w}) = \sum_{\nu=0}^{K-1} w_\nu |\phi_\nu\rangle\langle\phi_\nu|$ is a density matrix with a positive, decreasingly ordered spectrum, conveniently defined as $\boldsymbol{w} = (w_0, w_1, \ldots)$ with $w_\nu \geqslant w_{\nu+1} \geqslant 0$. The vectors $\{|\phi_\nu\rangle\}$ can be any set of K orthogonal states. Here $E_\nu \leqslant E_{\nu+1}$ are the exact eigenenergies of the system, arranged in increasing order. The ensemble variational principle in equation (5) offers a unified approach to variational methods in

quantum mechanics: the problem of the ground state is, in fact, just a particular case, corresponding to $\boldsymbol{w} = (1, 0, 0, \ldots)$. This variational approach to quantum excitations is currently playing a pivotal role in the extension of ground-state functional theories [31–35] and hybrid quantum–classical methods [15, 16, 36, 37] to excited states.

We note in passing that equation (5) can be written in a state-specific form by employing the purified state [38]:

$$|\rho(\boldsymbol{w})\rangle = \sum_{\nu=0}^{K-1} \sqrt{w_\nu}\, |\phi_\nu\rangle \otimes |a_\nu\rangle\,. \tag{6}$$

The states $|a_\nu\rangle$ are auxiliary orthonormal (ancilla) states added to perform the purification. The only condition is their orthornormality, $\langle a_\nu | a_\mu\rangle = \delta_{\nu\mu}$. Then, the lower bound of the energy expectation value of the ensemble energy can be written as $\langle\rho(\boldsymbol{w})|\hat{H}\otimes\mathbb{I}|\rho(\boldsymbol{w})\rangle \geqslant \boldsymbol{w}\cdot\boldsymbol{E}$, with $\boldsymbol{E} = (E_0, E_1, \ldots)$ and $\mathbb{I}$ being the identity matrix acting on the auxiliary space (we will skip the writing of $\mathbb{I}$ when the notation is obvious).

2.3. The ACSE for excited states

The generalization of the CSE to ensembles of eigenstates is straightforward. Indeed, since equation (2) is valid for all the eigenstates of the Hamiltonian $\hat{H}$, one can use it to write a weighted sum for the first K eigenstates: $\sum_{\nu=0}^{K-1} w_\nu \langle\psi_\nu|\hat{\Gamma}^{pq}_{st}(\hat{H} - E_\nu)|\psi_\nu\rangle = 0$. From this equation, the corresponding ACSE for an ensemble of K eigenstates follows:

$$\sum_{\nu=0}^{K-1} w_\nu \langle\psi_\nu| \left[\hat{\Gamma}^{pq}_{st}, \hat{H}\right] |\psi_\nu\rangle = 0\,. \tag{7}$$

This result suggests a variational implementation of the ACSE for excited states. Consider first a variational ansatz for a set of K orthogonal wave functions, iteratively constructed from unitary two-body exponential transformations:

$$|\phi_\nu^{(n+1)}\rangle = e^{\eta\hat{A}^{(n)}}|\phi_\nu^{(n)}\rangle\,, \tag{8}$$

where $\hat{A}^{(n)} = \sum_{pq,st} A^{(n)}_{pq,st}\hat{f}^\dagger_p\hat{f}^\dagger_q\hat{f}_t\hat{f}_s$ is an anti-Hermitian two-electron operator and η is a real positive number (whose role will be clear later). The ensemble energy at the $(n+1)$th iteration is the weighted sum of the energy expectation value of these states:

$$\mathcal{E}_{n+1} \equiv \sum_{\nu=0}^{K-1} w_\nu E_\nu^{(n+1)} = \sum_{\nu=0}^{K-1} w_\nu \langle\phi_\nu^{(n+1)}|\hat{H}|\phi_\nu^{(n+1)}\rangle\,. \tag{9}$$

Thus, at each iteration, the ensemble energy through order η is $\mathcal{E}_{n+1} = \mathcal{E}_n + \eta\sum_\nu w_\nu\langle\phi_\nu^{(n)}|[\hat{H}, \hat{A}^{(n)}]|\phi_\nu^{(n)}\rangle + \mathcal{O}(\eta^2)$. As in the case of the ground-state calculation [18], the gradient of the ensemble energy can be computed with respect to each $A^{(n)}_{pq,st}$:

$$\frac{\partial\mathcal{E}_n}{\partial A^{(n)}_{pq,st}} = \eta\sum_\nu w_\nu r^{(n)}_{\nu;pq,st}\,, \tag{10}$$

where $r^{(n)}_{\nu;pq,st} \equiv \langle\phi_\nu^{(n)}|[\hat{H}, \hat{\Gamma}^{pq}_{st}]|\phi_\nu^{(n)}\rangle$. This shows that the residual of the energy is the *weighted* expectation value of the commutators $[\hat{H}, \hat{\Gamma}^{pq}_{st}]$. The residual goes to zero when the ensemble is composed of eigenstates, which means that the ACSE in equation (7) is fulfilled. Hence, an algorithm to find the optimal operator $\hat{A}$ using gradient descent should perform the following update of the parameters at each step:

$$A^{(n+1)}_{pq,st} = -\eta\sum_\nu w_\nu \left\langle\phi_\nu^{(n)}\right| \left[\hat{H}, \hat{\Gamma}^{pq}_{st}\right] \left|\phi_\nu^{(n)}\right\rangle, \tag{11}$$

which implies that η can be interpreted as the learning rate of the algorithm.

Interestingly, the purification introduced in equation (6) can be used to write a more compact expression for the residual of the *ensemble* ACSE in equation (10), namely: $\langle\rho(\boldsymbol{w})|[\hat{\Gamma}^{pq}_{st}, \hat{H}]\otimes\mathbb{I}|\rho(\boldsymbol{w})\rangle$. If, in addition, one chooses the auxiliary states as a replica of the physical ones (i.e. $|a_\nu\rangle = |\phi_\nu\rangle$), then the state can be written as the following unitary transformation of the system's vacuum [38]: $|\rho(\boldsymbol{w})\rangle = V(\boldsymbol{w})|0\,\rangle$, where $V(\boldsymbol{w}) = UD(\boldsymbol{w})$, U is a unitary acting on the physical space and $D(\boldsymbol{w})$ is a squeezing operator acting on the duplicate Hilbert space of the system. More precisely, the operator reads $D(\boldsymbol{w}) = e^{G(\boldsymbol{w})}$, where

Algorithm 1. Parallelized CQE.

Given $K > 0$, $\boldsymbol{w} = (w_0, \ldots, w_{K-1})$, $\delta > 0$,
choose $0 < \eta < 1$,
choose K physical and ancilla states $\{|\phi_\nu\rangle, |a_\nu\rangle\}_{\nu=0}^{K-1}$,
initialize the state $|\rho_0(\boldsymbol{w})\rangle = \sum_{\nu=0}^{K-1} \sqrt{w_\nu}|\phi_\nu\rangle \otimes |a_\nu\rangle$.
Set $n \leftarrow 0$,
while $|A^{(n)}|^2 > \delta$ **do**
    prepare the state $|\Lambda_n^{\pm}\rangle = e^{\pm i\eta\hat{H}}|\rho_n(\boldsymbol{w})\rangle$,
    measure $A^{(n)}_{pq,st} = \frac{1}{2i}[\langle\Lambda_n^+|\hat{\Gamma}^{pq}_{st}|\Lambda_n^+\rangle - \langle\Lambda_n^-|\hat{\Gamma}^{pq}_{st}|\Lambda_n^-\rangle]$,
    prepare $|\Sigma_n(\theta)\rangle = \exp(\theta\hat{A}^{(n)})|\rho_n(\boldsymbol{w})\rangle$,
    minimize $\langle\Sigma_n(\theta)|\hat{H}|\Sigma_n(\theta)\rangle$ with respect to θ,
    take $\theta^* = \text{argmin}\langle\Sigma_n(\theta)|\hat{H}|\Sigma_n(\theta)\rangle$,
    prepare $|\rho_{n+1}(\boldsymbol{w})\rangle = \exp(\theta^*\hat{A}^{(n)})|\rho_n(\boldsymbol{w})\rangle$,
    $n \leftarrow n+1$.
end while

$G(\boldsymbol{w}) = \sum_m \theta_m(\hat{f}_m^\dagger\tilde{f}_m^\dagger - \tilde{f}_m\hat{f}_m)$ and $\cos(\theta_m) = \sqrt{1-w_m}$. As a result, the total residual can be written as a vacuum expectation value: $\langle 0|[\hat{\Gamma}^{pq}_{st}(\boldsymbol{w}), \hat{H}(\boldsymbol{w})]|0\rangle$, where the notation $\hat{A}(\boldsymbol{w}) = V^\dagger(\boldsymbol{w})\hat{A}V(\boldsymbol{w})$ is used. Hence, instead of evaluating the residual of several eigenstates and then summing this up as in equation (10), this result indicates that it is possible to work with only one specific state.

One possible way to implement the ACSE in a quantum device is to choose w_ν as fixed quantities and, for the $(n+1)$th iteration, allocate a certain number of shots N_ν to measure the contribution of $r_{\nu;pq,st}$ to the total residual in equation (10). Yet it is known that the most efficient way of deterministic assigning shots among the measurements consists of allocating N_ν proportionally to w_ν [39, 40]. But since the weights are not integers, this assignment results in a 'hard floor' on $N_{\text{total}} = \sum_\nu N_\nu \geqslant 1/w_K$ (recall that w_K is the minimum of the weights) [41]. This is the minimal number of shots needed for an unbiased estimate of the residuals of the ensemble $\sum_\nu w_\nu r^{(n)}_{\nu;pq,st}$. Unfortunately, for large K one can expect quite small w_K and therefore very large numbers of shots for each unbiased estimate. Random sampling can efficiently perform unbiased estimations of the residuals of the ensemble energy in equation (7) while using a cheap number of shots. In the next section, based on this sampling, we will present two quantum algorithms.

2.4. CQE for excited states

To introduce our algorithms, let us start first by choosing a set of weights $\boldsymbol{w}$, which for convenience we normalize to 1: $\sum_\nu w_\nu = 1$. Next, we choose K initial orthogonal states $|\phi_\nu\rangle$ that can be the K lowest mean-field (Hartree–Fock) wave functions. Weighted random sampling, where the probability of measuring r_ν is proportional to w_ν, can be used as an efficient unbiased estimator of the residuals of the ensemble energy in equation (7). A promising alternative to implementing this anti-Hermitian CQE that does not require a random number generator consists of preparing and measuring the purification presented in equation (6). For this *parallelized CQE* the initial state in equation (6) can be prepared by applying a suitable linear combination of unitaries [42] to the original Hartree–Fock state $|\rho_0\rangle = |\phi_{\text{HF}}\rangle \otimes |0, \ldots, 0\rangle$, with an ancilla term that uses only $\log_2 K$ qubits. At each iteration, the states $|\Lambda_n^{\pm}\rangle = \exp(\pm i\eta\hat{H})|\rho_n(\boldsymbol{w})\rangle$ are prepared and the entries of the matrix $A^{(n)}$ are measured from the equation

$$A^{(n)}_{pq,st} = \frac{1}{2i}\left(\langle\Lambda_n^+|\hat{\Gamma}^{pq}_{st}|\Lambda_n^+\rangle - \langle\Lambda_n^-|\hat{\Gamma}^{pq}_{st}|\Lambda_n^-\rangle\right) + \mathcal{O}\left(\eta^2\right).$$

Importantly, the residual in equation (10) is exactly zero for any set of eigenstates, not necessarily the lowest ones, so for any combination of eigenstates the optimization will stop at this point. Hence, to guarantee that the lowest set is found, we further prepare the state $|\Sigma_n(\boldsymbol{w})\rangle = \exp(\theta\hat{A}^{(n)})|\rho_n(\boldsymbol{w})\rangle$ and minimize the ensemble energy with respect to the value of θ. Besides circumventing local minima, this will also guarantee a faster convergence. As described in algorithm 1, the process is repeated until a desired convergence is reached.

Algorithm 2. Weighted random CQE.

Given $K > 0$, $\boldsymbol{w} = (w_0, \ldots, w_{K-1})$, $\sum_\nu w_\nu = 1$, $\delta > 0$,
choose $0 < \eta < 1$, and $N > 0$ number of shots,
choose K initial states $\{|\phi_0^{(0)}\rangle, \ldots, |\phi_{K-1}^{(0)}\rangle\}$,
Set $n \leftarrow 0$,
while $|A^{(n)}|^2 > \delta$ **do**
  $\boldsymbol{m} \sim \text{Multinomial}(N, \boldsymbol{w})$
  Set $A_{pq,st}^{(n)} \leftarrow 0$
  for $0 \leqslant \nu \leqslant K-1$ **do**
    for $1 \leqslant l \leqslant m_\nu$ **do**
      prepare $|\lambda_\nu^\pm\rangle = e^{\pm i\eta\hat{H}}|\phi_\nu^{(n)}\rangle$,
      $A_{pq,st}^{(n)} \leftarrow A_{pq,st}^{(n)} + \frac{1}{2i}\sum_{z=\pm} z\langle\lambda_\nu^z|\hat{\Gamma}_{st}^{pq}|\lambda_\nu^z\rangle$,
    end for
    prepare $|\Sigma_\nu(\theta)\rangle = e^{\theta\hat{A}^{(n)}}|\phi_\nu^n\rangle$,
  end for
  take $\theta^* = \text{argmin}\sum_\nu w_\nu\langle\Sigma_\nu(\theta)|\hat{H}|\Sigma_\nu(\theta)\rangle$,
  prepare $|\phi_\nu^{(n+1)}\rangle = \exp(\theta^*\hat{A}^{(n)})|\phi_\nu^{(n)}\rangle$,
  $n \leftarrow n+1$.
end while

We also sketch the *weighted random* CQE in algorithm 2. This algorithm follows similar lines as algorithm 1 except that the purification (or the parallelization) is replaced by assigning m_ν number of shots per state $|\phi_\nu\rangle$ randomly from a multinomial distribution: $\boldsymbol{m} \sim \text{Multinomial}(N_{\text{total}}, \boldsymbol{w})$. Because each of the excited states is treated separately, the algorithm is amenable to distributed parallel programming in which each state is prepared and measured on a separate quantum processor with the results only collected for the classical parts of the optimization. This weighted random sampling algorithm is *equivalent* to measuring the expectation value of the pure state $|\rho(\boldsymbol{w})\rangle$, in the sense that the variances of any observable computed by the two methods coincide. As a result, the number of shots needed to achieve a certain measurement error of the residuals is the same for both algorithms. Yet, while the results are certainly the same, the implementation clearly differs in the requirement of computational resources. An advantage, however, of the purification lies in the fact that quantum symmetries can easily be added to the cost function to improve convergence [43, 44].

Several advantages as well as similarities with respect to prior quantum algorithms for excited states are now apparent. For example, both the subspace-search VQE [15] and our parallelized CQEs share an important similarity: in both cases, the key idea is to ensure the orthogonality of the initial states $|\phi_\nu\rangle$ (i.e. $\langle\phi_\nu|\phi_\mu\rangle = \delta_{\nu\mu}$) at the input of the quantum circuit, rather than at the output. Yet, in contrast to many previously published VQE-inspired algorithms (e.g. [10, 13–17]), our CQE algorithms do not identify an energy cost function to be minimized by classical means but a residual that guides the parameters of a unitary towards the ones that transform the input states into the desired set of eigenstates. Moreover, by construction, in CQE the number of variational parameters is fixed by the total number of two-body parameters present in the Hamiltonian which ensures the scalability of the algorithm.

3. Results

We now present the results of both algorithms when applied to model and molecular Hamiltonians and discuss their advantages and disadvantages. The first system we investigate with the ensemble ACSE is the generic M-qubit Hamiltonian:

$$\hat{H} = \sum_{r_1=0}^{3}\cdots\sum_{r_M=0}^{3}\lambda_{r_1,\ldots,r_M}\sigma_{r_1}\otimes\cdots\otimes\sigma_{r_M}\,, \tag{12}$$

where σ_n denotes the Pauli matrix. The initial state is denoted as $|\rho_0(\boldsymbol{w})\rangle = \sum_{\boldsymbol{i}\in\{0,1\}^M}\sqrt{w_{\boldsymbol{i}}}\,|\boldsymbol{i}\rangle_p\otimes|\boldsymbol{i}\rangle_a$, where p/a denotes the physical/ancilla qubits and $\boldsymbol{i} = (i_1, \ldots, i_M)$. The evolution into the exact eigenstates for a random Hamiltonian of the form in equation (12) for systems sizes $M = 2, 3$ is presented in figure 1. We chose the learning rate $\eta = 0.3$ and weights $\boldsymbol{w} = (M^2, M^2-1, \ldots, 1)$ and then $\boldsymbol{w} \to \boldsymbol{w}/\sum_i w_i$. For $M = 2$ and a random choice of the 16 parameters λ_{r_1,r_2}, the ground state is reached in 8 iterations, while the exact eigenstate calculation is reached in 20. The two highest energy states, having the lowest weights in the cost function, converge the slowest, and, due to orthogonality limiting the degrees of freedom, converge simultaneously. A similar pattern can be seen for another random Hamiltonian for the case $M = 3$, and a random choice of the 64 parameters λ_{r_1,r_2,r_3}, but due to the larger dimension of the Hilbert space, more

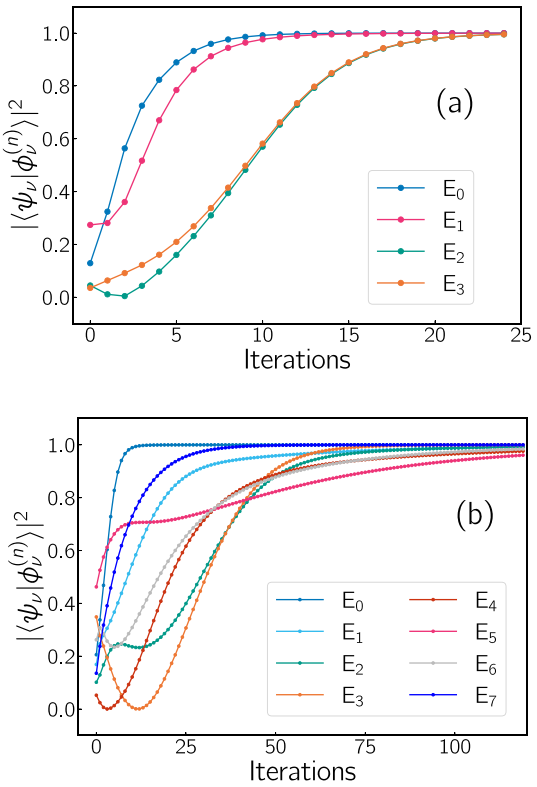

Figure 1. Evolution of the projection of the states $|\phi_\nu^{(n)}\rangle$ on the exact eigenstates $|\psi_\nu\rangle$ as a function of the iteration n for (a) 2-qubit and (b) 3-qubit random Hamiltonians in equation (12).

iterations are needed for convergence. We note that, in this example, the number of terms of the Hamiltonian scales as 2^{2M}. Yet, by restricting the set of variational parameters to be real, the relevant operators entering in the ACSE unitary (11) correspond to the elements of the Lie algebra $o(2^M)$ whose dimension is $2^M(2^M-1)/2$.

We investigate also two molecular examples: (a) a noisy backend simulation of H_2 and (b) a noiseless state-vector simulation of H_4. All calculations were performed using the minimal Slater-type orbital (STO-3G) basis set. The noisy backend is the FakeLagosV2, which is one of the fake backends that mimic the behavior of the IBM quantum computers using system snapshots [45]. The statevector simulator output is extracted without sampling error.

The calculation of H_2 is performed in the spin-symmetry sector $S_z = 0$, the learning rate is chosen as $\eta = 0.1$ and θ is determined from a quick linear search, sketching ten energy points with $\theta = 0.1, 0.2, 0.3, \ldots, 1.0$. Based on the symmetry of the problem, we construct the Hamiltonian in a compressed form with two qubits. Two additional ancillary qubits are used to create the purified ensemble of all four eigenstates, resulting in four qubits in total. The detailed circuit preparation has been reported in previous work [46]. For the single-point calculation in figure 2, performed with the parallel CQE, the ensemble energy converges to a minimum in only three iterations. Remarkably, we achieve an error of less than 30 mHartree for each state without any error mitigation techniques. We also present the dissociation curve of H_2 in figure 2. Energies computed from parallel CQE are in excellent agreement with the full CI results with an average mean unsigned error of 26 mHartree (without error mitigation). To give an idea of what this error means, recall that the noisy backend we are using is not an analytical noise model, but a mimic of a real quantum system which, even for preparing unmixed Slater determinants and measuring the corresponding energy, yields an average error of around 20 mHartree.

It is also worth discussing the role weight values w_i play in the rate of convergence. For instance, if all of the weights are equal, only an eigen-subspace can be found, and the individual eigenstates would have to be resolved with classical diagonalization. Giving different values for the weights allows us to perform the entire calculation on a quantum device, resulting in a faster convergence. Indeed, we find that the optimal convergence for H_2 (presented in figure 2) is achieved with the weights $\boldsymbol{w} \sim (9, 9, 1, 1)$, before normalization. To explain our choice, let us observe that, due to the system's point-group symmetry, the Hamiltonian matrix is block diagonal with two 2×2 sub-matrices on the diagonal. Therefore, since the minimization runs

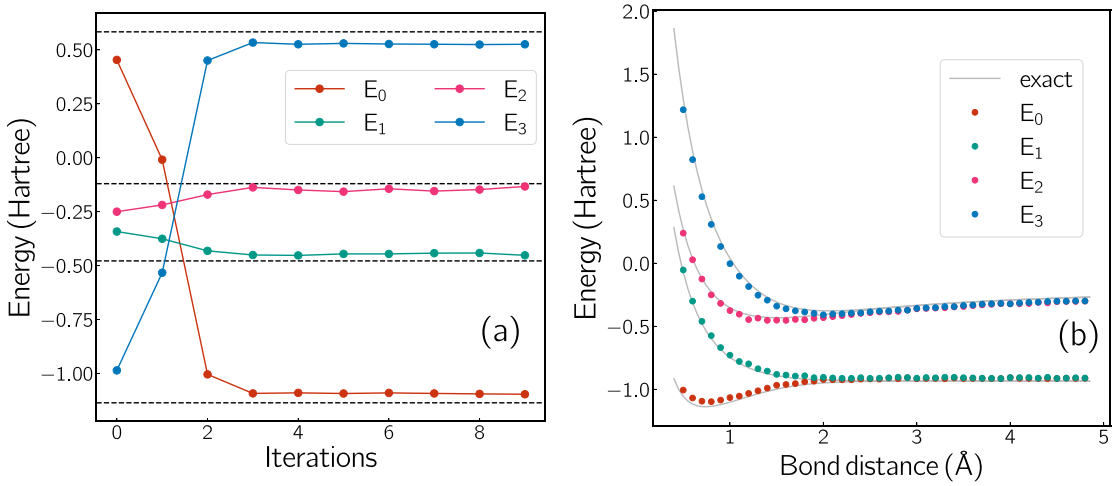

Figure 2. (a) Obtained energies during the optimization for single point calculation of H_2 (bond distance of 0.7 Å). The exact solutions for each state and the ensemble are indicated by black dashed lines. (b) Energies along the dissociation curve computed from 0.5 to 5 Å. The exact results are shown as black lines and our single-point calculations are shown as dots.

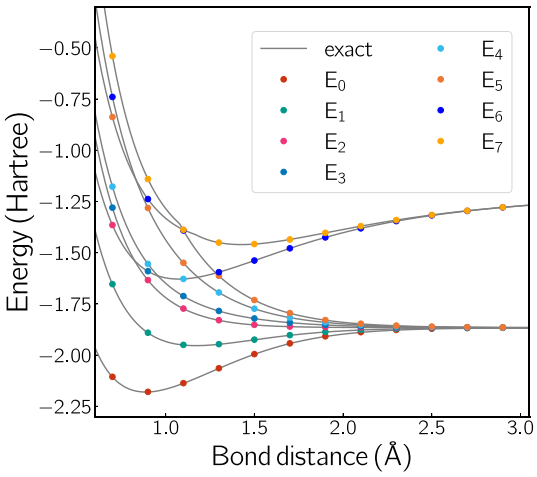

Figure 3. The computed and exact lowest eight eigenenergies of the linear equidistant H_4 as a function of the H-H distance.

independently within each sub-block, we opted for two identical pairs of weights. This indicates that the optimal choice of weights is highly dependent on the molecular symmetries.

Linear H_4 is a widely used benchmark system for strong correlation in electronic structure theory [44, 47]. As the molecule dissociates, the energy levels become highly degenerate due to the non-interacting hydrogen atoms and the system exhibits significant static correlation [48]. We take the equidistant form of linear H_4 and use the Jordan–Wigner transformation to map the Hamiltonian from four spatial orbitals to eight qubits. Both algorithms 1 and 2 successfully find the ground and excited states. Yet in the first case, as we are tackling eight states simultaneously, one requires at least three ancillary qubits to prepare all initial states in the expanded Hilbert space. Alternatively, preparing different initial states separately and sampling them using a multinomial distribution (as in our algorithm 2) becomes particularly valuable with limited qubit resources or when the ancilla-based preparations are hard to perform.

For the calculation of H_4 shown in figure 3, we have used the weight vector $(8, 7, \ldots, 1)$, before normalization, and $\eta = 0.000\,001$. At a long bond distance, we seed the eight initial guesses with the eight single Slater determinants with the lowest energies. Afterward, each state in the calculation is seeded with the two most important Slater determinants of the corresponding state found in the previous calculation. While the potential energy curves are highly degenerate towards dissociation, as the bond begins the form, the energy curves separate. As shown in figure 3, for the dissociation curve on a noiseless simulator, our algorithms give almost exact results (i.e. an error of around 10^{-4} Hartree). Most calculations converged in less than 200 iterations. We recall that this convergence speed does depend on the weight being assigned to

each element, the initial guess, as well as the optimization method, suggesting opportunities for further exploration and improvement.

4. Conclusions

In this paper, we have combined CQE, originally developed for the calculation of molecular ground states, and the Rayleigh–Ritz variational principle for ensemble states into an excited-state CQE. Quite remarkably, our scheme allows us to compute simultaneously an arbitrary number of lowest eigenstates while preserving the favorable scaling and ease of implementation of the ground-state CQE. Unlike approaches based on the unitary coupled cluster and related ansätze, that give an approximation to the cost function, our algorithm provides a natural choice for the unitary operator through the measured residual. In our experiments with molecular and model systems, we tackle multiple states simultaneously with excellent accuracy in both the weakly and strongly correlated regimes. The ability to optimize near-degenerate states by assigning different weights allows us to study both near-degeneracy and conical intersections, which can be used for nonadiabatic chemistry. An interesting question for the future is how to use our algorithms for excited states and spectroscopy when additional bosonic degrees are present. Finally, while we did not perform any particular circuit optimization, it will be important to investigate how compact circuits can be produced for excited state calculation in a similar fashion as is being done for ground states [49, 50].

Data availability statement

The data that support the findings of this study are openly available at the following URL/DOI: https://github.com/damazz/Parallel-CQE. All codes to reproduce, examine, and improve our proposed analysis are freely available online [51].

Acknowledgments

C L B-R gratefully acknowledge financial support from the European Union's Horizon Europe Research and Innovation program under the Marie Skłodowska-Curie Grant Agreement No. 101065295. Views and opinions expressed are however those of the authors only and do not necessarily reflect those of the European Union or the European Research Executive Agency. D A M gratefully acknowledges the U.S. Department of Energy, Office of Basic Energy Sciences, Grant DE-SC0019215 and the U.S. National Science Foundation Grant No. CHE-2155082.

ORCID iDs

Carlos L Benavides-Riveros https://orcid.org/0000-0001-6924-727X
Yuchen Wang https://orcid.org/0000-0003-0479-3776
Samuel Warren https://orcid.org/0000-0001-5713-4454
David A Mazziotti https://orcid.org/0000-0002-9938-3886

References

[1] Cerezo M *et al* 2021 Variational quantum algorithms *Nat. Rev. Phys.* **3** 625
[2] Bauman N *et al* 2021 Toward quantum computing for high-energy excited states in molecular systems: quantum phase estimations of core-level states *J. Chem. Theory Comput.* **17** 201
[3] O'Malley P *et al* 2016 Scalable quantum simulation of molecular energies *Phys. Rev.* X **6** 031007
[4] Sugisaki K, Yamamoto S, Nakazawa S, Toyota K, Sato K, Shiomi D and Takui T 2016 Quantum chemistry on quantum computers: a polynomial-time quantum algorithm for constructing the wave functions of open-shell molecules *J. Phys. Chem.* A **120** 6459
[5] Hempel C *et al* 2018 Quantum chemistry calculations on a trapped-ion quantum simulator *Phys. Rev.* X **8** 031022
[6] Abrams D S and Lloyd S 1999 Quantum algorithm providing exponential speed increase for finding eigenvalues and eigenvectors *Phys. Rev. Lett.* **83** 5162
[7] Aspuru-Guzik A, Dutoi A D, Love P J and Head-Gordon M 2005 Simulated quantum computation of molecular energies *Science* **309** 1704
[8] Peruzzo A, McClean J, Shadbolt P, Yung M-H, Zhou X-Q, Love P J, Aspuru-Guzik A and O'Brien J L 2014 A variational eigenvalue solver on a photonic quantum processor *Nat. Commun.* **5** 4213
[9] McClean J R, Romero J, Babbush R and Aspuru-Guzik A 2016 The theory of variational hybrid quantum-classical algorithms *New J. Phys.* **18** 023023
[10] Higgott O, Wang D and Brierley S 2019 Variational quantum computation of excited states *Quantum* **3** 156
[11] Jones T, Endo S, McArdle S, Yuan X and Benjamin S C 2019 Variational quantum algorithms for discovering Hamiltonian spectra *Phys. Rev.* A **99** 062304
[12] Ibe Y, Nakagawa Y O, Earnest N, Yamamoto T, Mitarai K, Gao Q and Kobayashi T 2022 Calculating transition amplitudes by variational quantum deflation *Phys. Rev. Res.* **4** 013173

[13] Wen J, Lv D, Yung M-H and Long G-L 2021 Variational quantum packaged deflation for arbitrary excited states *Quantum Eng.* **3** e80
[14] Shirai S, Horiba T and Hirai H 2022 Calculation of core-excited and core-ionized states using variational quantum deflation method and applications to photocatalyst modeling *ACS Omega* **7** 10840
[15] Nakanishi K M, Mitarai K and Fujii K 2019 Subspace-search variational quantum eigensolver for excited states *Phys. Rev. Res.* **1** 033062
[16] Yalouz S, Senjean B, Günther J, Buda F, O'Brien T and Visscher L 2021 A state-averaged orbital-optimized hybrid quantum–classical algorithm for a democratic description of ground and excited states *Quantum Sci. Technol.* **6** 024004
[17] Tilly J *et al* 2022 The variational quantum eigensolver: a review of methods and best practices *Phys. Rep.* **986** 1
[18] Smart S E and Mazziotti D A 2021 Quantum solver of contracted eigenvalue equations for scalable molecular simulations on quantum computing devices *Phys. Rev. Lett.* **126** 070504
[19] Mazziotti D A 2004 Exactness of wave functions from two-body exponential transformations in many-body quantum theory *Phys. Rev.* A **69** 012507
[20] Wang Y and Mazziotti D A 2023 Electronic excited states from a variance-based contracted quantum eigensolver *Phys. Rev.* A **108** 022814
[21] Smart S E, Welakuh D M and Narang P 2023 Many-body excited states with a contracted quantum eigensolver (arXiv:2305.09653 [quant-ph])
[22] Mazziotti D A 2007 Anti-Hermitian part of the contracted Schrödinger equation for the direct calculation of two-electron reduced density matrices *Phys. Rev.* A **75** 022505
[23] Nakatsuji H 1976 Equation for the direct determination of the density matrix *Phys. Rev.* A **14** 41
[24] Mazziotti D A 1998 Contracted Schrödinger equation: determining quantum energies and two-particle density matrices without wave functions *Phys. Rev.* A **57** 4219
[25] Mazziotti D A 2007 Contracted Schrödinger equation *Reduced-Density-Matrix Mechanics: with Application to Many-Electron Atoms and Molecules* (Wiley) ch 8, pp 165–203
[26] Mazziotti D A 2006 Anti-Hermitian contracted Schrödinger equation: direct determination of the two-electron reduced density matrices of many-electron molecules *Phys. Rev. Lett.* **97** 143002
[27] Valdemoro C, Tel L, Alcoba D and Pérez-Romero E 2007 The contracted Schrödinger equation methodology: study of the third-order correlation effects *Theor. Chem. Account.* **118** 503
[28] Wang Y, Smith L M and Mazziotti D A 2023 Quantum simulation of bosons with the contracted quantum eigensolver *New J. Phys.* **25** 103005
[29] Kryloff N 1931 *Les Méthodes de Solution Approchée des Problèmes de la Physique Mathématique* (*Mémorial des Sciences Mathématiques*) (Gauthier-Villars)
[30] Gross E K U, Oliveira L N and Kohn W 1988 Density-functional theory for ensembles of fractionally occupied states. I. Basic formalism *Phys. Rev.* A **37** 2809
[31] Fromager E 2020 Individual correlations in ensemble density functional theory: state- and density-driven decompositions without additional Kohn-Sham systems *Phys. Rev. Lett.* **124** 243001
[32] Marut C, Senjean B, Fromager E and Loos P 2020 Weight dependence of local exchange-correlation functionals in ensemble density-functional theory: double excitations in two-electron systems *Faraday Discuss.* **224** 402
[33] Schilling C and Pittalis S 2021 Ensemble reduced density matrix functional theory for excited states and hierarchical generalization of Pauli's exclusion principle *Phys. Rev. Lett.* **127** 023001
[34] Gould T, Kooi D P, Gori-Giorgi P and Pittalis S 2023 Electronic excited states in extreme limits via ensemble density functionals *Phys. Rev. Lett.* **130** 106401
[35] Cernatic F, Senjean B, Robert V and Fromager E 2021 Ensemble density functional theory of neutral and charged excitations *Top. Curr. Chem.* **380** 4
[36] Xu G, Guo Y B, Li X, Wang K, Fan Z, Zhou Z S, Liao H J and Xiang T 2023 Concurrent quantum eigensolver for multiple low-energy eigenstates *Phys. Rev.* A **107** 052423
[37] Han Z *et al* 2024 Multilevel variational spectroscopy using a programmable quantum simulator *Phys. Rev. Res.* **6** 013015
[38] Benavides-Riveros C L, Chen L, Schilling C, Mantilla S and Pittalis S 2022 excitations of quantum many-body systems via purified ensembles: a unitary-coupled-cluster-based approach *Phys. Rev. Lett.* **129** 066401
[39] Rubin N, Babbush R and McClean J 2018 Application of fermionic marginal constraints to hybrid quantum algorithms *New J. Phys.* **20** 053020
[40] Yen T-C, Ganeshram A and Izmaylov A F 2023 Deterministic improvements of quantum measurements with grouping of compatible operators, non-local transformations and covariance estimates *npj Quantum Inf.* **9** 14
[41] Arrasmith A, Cincio L, Somma R and Coles P 2020 Operator sampling for shot-frugal optimization in variational algorithms (arXiv:2004.06252 [quant-ph])
[42] Childs A M and Wiebe N 2012 Hamiltonian simulation using linear combinations of unitary operations *Quantum Inf. Comput.* **12** 901
[43] Pollmann F, Khemani V, Cirac J I and Sondhi S L 2016 Efficient variational diagonalization of fully many-body localized Hamiltonians *Phys. Rev.* B **94** 041116
[44] Lyu C, Xu X, Yung M-H and Bayat A 2023 Symmetry enhanced variational quantum spin eigensolver *Quantum* **7** 899
[45] Qiskit Contributors 2023 Qiskit: an open-source framework for quantum computing (https://doi.org/10.5281/zenodo.2573505)
[46] Hong C-L, Colmenarez L, Ding L, Benavides-Riveros C L and Schilling C 2023 Quantum parallelized variational quantum eigensolvers for excited states (arXiv:2306.11844 [quant-ph])
[47] Zhang F, Gomes N, Berthusen N F, Orth P P, Wang C-Z, Ho K-M and Yao Y-X 2021 Shallow-circuit variational quantum eigensolver based on symmetry-inspired hilbert space partitioning for quantum chemical calculations *Phys. Rev. Res.* **3** 013039
[48] Benavides-Riveros C L, Lathiotakis N N and Marques M A L 2017 Towards a formal definition of static and dynamic electronic correlations *Phys. Chem. Chem. Phys.* **19** 12655
[49] Cao C, Hu J, Zhang W, Xu X, Chen D, Yu F, Li J, Hu H, Lv D and Yung M 2022 Progress toward larger molecular simulation on a quantum computer: simulating a system with up to 28 qubits accelerated by point-group symmetry *Phys. Rev.* A **105** 062452
[50] Fan Y, Cao C, Xu X, Li Z, Lv D and Yung M 2023 Circuit-depth reduction of unitary-coupled-cluster ansatz by energy sorting *J. Phys. Chem. Lett.* **14** 9596
[51] Benavides-Riveros C L, Wang Y , Warren S and Mazziotti D A 2023 Quantum simulation of excited states from parallel contracted quantum eigensolvers (available at: https://github.com/damazz/Parallel-CQE)